Stokes Shift Dynamics in Ionic Liquids: Temperature Dependence

Hemant K. Kashyap and Ranjit Biswas*

Department of Chemical, Biological & Macromolecular Sciences, S. N. Bose National Centre for Basic Sciences, JD Block, Sector III, Salt Lake, Kolkata 700 098, India

Received: July 7, 2010; Revised Manuscript Received: November 4, 2010

A recently developed molecular theory is used to investigate the temperature dependence of the dynamic fluorescence Stokes shift of a dipolar solute in seven imidazolium ionic liquids. The temperature range considered is 278.15−338.15 K, for which experimental dielectric relaxation data (frequency range of $0.2 \leq \nu/\mathrm{GHz} \leq 89$) are available. The theory used here explores and substantiates the relation between fluorescence spectral dynamics and dielectric relaxation in ionic liquids. The slope of the temperature-dependent change in the calculated total dynamic Stokes shift is predicted to follow an inverse-linear correlation with that (slope) of the experimentally measured temperature dependence of the static dielectric constant of these liquids. This explains the experimentally observed decrease of polarity parameter, $E_T(30)$, with temperature for several different ionic liquids. A significant part of the stabilization energy of a dissolved excited dipolar solute is found to arise from the reorientational dynamics of the dipolar ions (mainly imidazolium cations) of these liquids. The separated solute−solvent dipole−ion interaction contribution to the shift exhibits a stronger temperature dependence than the dipole−dipole interaction component. Calculations predict bimodal Stokes shift dynamics for all of these liquids with a fast initial component arising from rapid angular adjustment of the dipolar ions. The slow, stretched-exponential component shows a systematic temperature dependence and is linked to an environment rearrangement through the center-of-mass motion of the ions. Subsequently, calculated solvation activation energies are found to be closely related to those observed in the corresponding conductivity and viscosity measurements for these ionic liquids.

I. Introduction

Recent years have witnessed intense activity in investigating solute−solvent interactions and solvent dynamics in room-temperature ionic liquids.[1−10] Both fluorescence spectroscopic measurements and computer simulation studies have been employed to generate a molecular-level understanding of the interactions and dynamics in this new class of solvents. Apart from technological relevance and possible industrial applications,[11−13] the very basic scientific aspects of how dynamically different these liquids are from the well-studied conventional polar solvents, as well as implications of these differences for simple chemical events in the solution phase, have provided much of the motivation to the researchers in this field. Because ion−ion Coulomb interactions largely govern both the structure and dynamics of ionic liquids, the medium response to an external perturbation is expected to be different for these liquids than for those where dipolar interactions dominate the relaxation processes.[14] In fact, dynamic fluorescence Stokes shift measurements have revealed a qualitative difference between room-temperature ionic liquids and ambient polar solvents and signaled a breakdown of dielectric-relaxation-based theories that were otherwise successful in explaining the experimental Stokes shift dynamics in conventional polar solvents.[3] Despite the presence of a good body of experimental results on Stokes shift dynamics in room-temperature ionic liquids and fused inorganic salts, developing a molecular theory at the level of existing theories for dipolar solvents has remained a challenge. The presence of longer-ranged charge−charge interactions, microscopic heterogeneity (spatial and temporal),[15−21] and the possibility of the presence of multiple species in a given ionic liquid have made the task quite nontrivial.

A survey of the existing Stokes shift data reveals that, even though measurements have been carried out to characterize the solvation response in many ionic liquids with a large combination of anions and alkylated cations, systematic temperature-dependent measurements are not as plentiful. The few measurements that exist, nonetheless, provide useful information about solute−solvent coupling by probing the viscosity dependence of either average solvation or rotation times.[22−28] Very recently, temperature-dependent dielectric relaxation measurements for a few imidazolium ionic liquids have been carried out that find the relaxation process at low frequency to derive contributions from both single-particle rotation and cooperative motions.[28] These data, therefore, indicate important roles for the dipolar rotation and collective motions of the solvent particles in dictating the Stokes shift dynamics in these ionic liquids, provided that a relationship exists between the frequency-dependent dielectric function and the solvation response in these liquids. The recently developed semimolecular theory,[29−31] which connects the solvation response in ionic liquids to the measured dielectric relaxation data much the same way as in neat polar solvents,[32−36] is employed here to predict the temperature dependence of the Stokes shift and its dynamics in several imidazolium ionic liquids.

We have chosen the well-known solvation probe coumarin 153 (C153)[37] as a dipolar solute and studied Stokes shift dynamics in the following ionic liquids: 1-*N*-butyl-3-*N*-methylimidazolium hexafluorophosphate ([bmim][PF_6]) and the corresponding tetrafluoroborate ([bmim][BF_4]) and dicynamide ([bmim][DCA]), 1-*N*-ethyl-3-*N*-methylimidazolium tetrafluoroborate ([emim][BF_4]) and its dicynamide ([emim][DCA]), and 1-*N*-

* To whom correspondence should be addressed. E-mail: ranjit@bose.res.in.

10.1021/jp106271n
Published on Web 12/02/2010

hexyl-3-*N*-methylimidazolium tetrafluoroborate ([hmim][BF_4]) and its [bis(trifluoromethylsulfonyl)imide] analogue ([hmim][NTf_2]). As already discussed, these liquids are chosen because of the existence of experimental dielectric relaxation data for these liquids. Because the present theory separates the total dynamic Stokes shift into solute−solvent dipole−dipole and dipole−ion contributions,[30] it would be interesting to investigate which of these two responds more strongly to the temperature variation. Theoretical results obtained here can be used to predict which of the ionic liquids—dipolar or nondipolar—is likely to exhibit a stronger temperature dependence. The predicted results can then be re-examined by performing conventional dynamic Stokes shift experiments.

The rest of this article is organized as follows: The molecular theory used here is briefly described in the next section, where the computational details are also summarized. Numerical results are presented in section III. A comparison between the theoretical predictions and the existing experimental results are also provided in this section. The article then ends with a discussion in section IV.

II. Theoretical Formulation and Calculation Details

A. Derivation of Necessary Expressions. Because the microscopic theory used here has already been described in detail elsewhere,[29−31] we briefly discuss here the theory, the assumptions required to derive the semianalytical expressions, and the method of calculations of the relevant quantities from those microscopic equations.

For a dipolar solute dissolved in an imidazolium ionic liquid, the theory used here considers the presence of the following interactions: (i) dipole−dipole interactions between dipolar solvent ions, (ii) ion−ion interactions between solvent ions, (iii) dipole−dipole interactions between the dissolved dipolar solute and dipolar solvent ion, and (iv) dipole−ion interactions between the solute and solvent ions. Solute−solute interactions are ignored because, in experiments, often very dilute solutions ($\leq 10^{-5}$ mol/L) of probe molecules are used.[37,38] In addition, interactions due to the presence of ion-pair and higher ion aggregates[39,40] are completely neglected in this theory. This is an approximation required to preserve the analytical simplicity of the present formalism, but it can affect the predictability because each of these interactions could contribute to the experimental measurements. In conventional Stokes shift experiments of dipolar (such as imidazolium) ionic liquids, however, the solute−solvent dipole−dipole and dipole−ion interactions are the principal contributors to the total solvent stabilization of the laser-excited dipolar probe, whereas the solvent stabilization time scale is mainly governed by the dynamics of solvent−solvent dipolar and ion−ion interactions. The ion−dipole interactions between solvent molecules in dipolar ionic liquids represent another component that can also contribute to the experimentally measured time scale of solvent rearrangement, but the present theory does not include the cross-interactions, arguing that the density fluctuation time scales for the dipolar and ionic species are very different from each other and thus uncorrelated. Although such a separation might not exist in real solutions because the motions of the dipolar and ionic species are adiabatically coupled,[41−44] dynamic Stokes shift measurements indicate that the effects of ion motion appear at longer times in the dynamic response of electrolyte solutions.[38] Therefore, the present theory is an approximate general framework for studying Stokes shift dynamics in both ionic liquids and electrolyte solutions where the above four interactions are expected to dominate.

For a solute−solvent system with the interactions described above, it is now possible to use the classical density functional theory to write an expression for the free energy functional ($\Delta\beta F_{int}$, with $\beta = 1/k_BT$) in terms of position- (**r**-) and orientation- ($\mathbf{\Omega}$-) dependent densities of dipolar cation, dipolar solute, and position-dependent anion in the solution.[45,46] Then, equating the functional derivative of $\Delta\beta F_{int}$ with respect to the solute density to zero (equilibrium property) provides the expression for the average interaction experienced by a dipolar solute molecule immersed in such a solution. Subsequent extension into the time domain allows one to derive the following expression for the time- (*t*-), position-, and orientation-dependent solvation energy for a mobile dipolar solute[29−31]

$$\Delta E_{total}(\mathbf{r},\mathbf{\Omega};t) = -k_BT\rho_s(\mathbf{r},\mathbf{\Omega};t)\times \left[\int d\mathbf{r}'\, d\mathbf{\Omega}'\, c_{sd}(\mathbf{r},\mathbf{\Omega};\mathbf{r}',\mathbf{\Omega}')\,\delta\rho_d(\mathbf{r}',\mathbf{\Omega}';t) + \sum_{\alpha=1}^{2}\int d\mathbf{r}'\, c_{s\alpha}(\mathbf{r},\mathbf{\Omega};\mathbf{r}')\,\delta n_\alpha(\mathbf{r}';t)\right] = \Delta E_{sd}(\mathbf{r},\mathbf{\Omega};t) + \Delta E_{si}(\mathbf{r},\mathbf{\Omega};t) \quad (1)$$

where $\rho_s(\mathbf{r},\mathbf{\Omega};t)$ is the solute density at position **r** with orientation $\mathbf{\Omega}$ at any time *t*. $c_{sd}(\mathbf{r},\mathbf{\Omega};\mathbf{r}',\mathbf{\Omega}')$ and $c_{s\alpha}(\mathbf{r},\mathbf{\Omega};\mathbf{r}')$ are the position- and orientation-dependent dipolar solute−dipolar ion and dipolar solute−ion direct correlation functions, respectively, and α denotes the type of ions (cation and anion). The fluctuations in dipolar density ($\delta\rho_d$) and ion density (δn_α) from the corresponding bulk values are defined as follows: $\delta\rho_d(\mathbf{r},\mathbf{\Omega}) = \rho_d(\mathbf{r},\mathbf{\Omega}) - \rho_d^0/4\pi$ and $\delta n_\alpha(\mathbf{r}) = n_\alpha(\mathbf{r}) - n_\alpha^0$. Equation 1 expresses the total solvation energy $\Delta E_{total}(\mathbf{r},\mathbf{\Omega};t)$ as a sum of two distinct contributions: one due to the dipole−dipole interaction, $\Delta E_{sd}(\mathbf{r},\mathbf{\Omega};t)$, and the other due to the dipole−ion interaction, $\Delta E_{si}(\mathbf{r},\mathbf{\Omega};t)$. Such a summation of two independent interaction contributions arises from the linearization of $\Delta\beta F_{int}$ in terms of dipolar and ionic density fluctuations ($\delta\rho_d$ and δn_α). This linearization also suggests that the pure dipolar solvent structure and dynamics are not perturbed by the presence of either the solute or the dispersed ions. However, these approximations have been found not to affect the qualitative description of the experimental Stokes shift dynamics in polar media and dipolar ionic liquids mainly because of the dominance of the collective solvent modes.[29,30]

The time-dependent fluctuating total solvation energy (fluctuation from the equilibrium value) autocorrelation function is then approximated as[30]

$$\langle \Delta E_{total}(t)\,\Delta E_{total}(t')\rangle = \langle \Delta E_{sd}(t)\,\Delta E_{sd}(t')\rangle + \langle \Delta E_{si}(t)\,\Delta E_{si}(t')\rangle \quad (2)$$

where the cross-correlations between the fluctuating dipole−dipole and ion−dipole interaction contributions have been neglected, assuming that the fluctuating time scales of these quantities are widely different from each other. Within such an approximation, eq 2 expresses the total solvation energy time autocorrelation function as a sum of individual autocorrelation functions: dipole−dipole and dipole−ion interaction energy time autocorrelations. Note that such a separation might not exist in real electrolyte solutions, as equilibrium ion-density fluctuation is expected to be coupled to dipolar density fluctuation. Because orientational polarization density relaxation is much faster for

common polar solvents, the time scales associated with the fluctuations in the dipolar and ion densities are different from each other. However, this separation is only semiquantitative, as ion motion would always involve solvent motion and vice versa.[38,41−44]

The normalized solvation energy time autocorrelation function then describes the time dependence of the solvation energy relaxation[30]

$$S_E(t) = \frac{\langle|\Delta E_{sd}(0)|^2\rangle S_{sd}(t)}{\langle|\Delta E_{sd}(0)|^2\rangle + \langle|\Delta E_{si}(0)|^2\rangle} + \frac{\langle|\Delta E_{si}(0)|^2\rangle S_{si}(t)}{\langle|\Delta E_{sd}(0)|^2\rangle + \langle|\Delta E_{si}(0)|^2\rangle} \quad (3)$$

with $S_{sd}(t)$ denoting the normalized solvation energy time autocorrelation functions due to solute−solvent dipolar interactions and $S_{si}(t)$ denoting that due to solute−ion (dipole−ion) interactions. According to this formalism, therefore, the total solvation energy relaxes through two separate channels. Although the faster channel dominates the total decay, the average rate of the decay is governed by the slower channel. It is well-known that, in the linear response regime, $S_E(t)$ is assumed to be equivalent to the solvation response function, $S(t)$, measured in dynamic Stokes shift experiments. Consequently, comparison of the predicted results with experimental data is done within the purview of this approximation.

B. Calculation of the Solute−Solvent Dipolar Interaction Contribution, $S_{sd}(t)$. The relevant expression for the normalized solvation energy autocorrelation function due to the dipole−dipole interaction has been shown to be given by[30]

$$S_{sd}(t) = \frac{\langle \Delta E_{sd}(t)\, \Delta E_{sd}(0)\rangle}{\langle|\Delta E_{sd}(0)|^2\rangle} = \frac{P\int_0^\infty dk\, k^2 S^{10}_{solute}(k;t)\,|c^{10}_{sd}(k)|^2\, S^{10}_{solvent}(k;t) + 2P\int_0^\infty dk\, k^2 S^{11}_{solute}(k;t)\,|c^{11}_{sd}(k)|^2\, S^{11}_{solvent}(k;t)}{P\int_0^\infty dk\, k^2 S^{10}_{solute}(k)\,|c^{10}_{sd}(k)|^2\, S^{10}_{solvent}(k) + 2P\int_0^\infty dk\, k^2 S^{11}_{solute}(k)\,|c^{11}_{sd}(k)|^2\, S^{11}_{solvent}(k)} \quad (4)$$

where the prefactor is $P = 2\rho_d^0(k_BT/2\pi)^2$, $c^{lm}_{sd}(k)$ denotes the Fourier transform of the (l, m) component of the static correlation function between the solute and dipolar ionic liquid species, and $S^{lm}_{solvent}(k,t)$ is the same component of the wavevector- (k-) dependent orientational dynamic structure factor of the dipolar ionic liquid. The calculation of $S^{lm}_{solvent}(k,t)$ requires as inputs (i) the orientational static structure factor, (ii) the experimental dielectric relaxation data of these ionic liquids, and (iii) the isotropic liquid dynamic structure factor.[29−36] These are necessary to calculate the wavevector- and frequency- (z-) dependent rotational and translational memory kernels, namely, $\Gamma_R(k,z)$ and $\Gamma_T(k,z)$, that constitute $S^{lm}_{solvent}(k,t)$. The orientational static structure factor for these ionic liquids is obtained from the mean spherical approximation (MSA) model[47] with proper corrections at both $k \to 0$ and $k \to \infty$ limits, using the experimental static dielectric constant after approximating the dipolar species as dipolar hard spheres. The dipole moment of the ionic liquid at each temperature was estimated according to the experimental static dielectric constant, and the room-temperature value was found to be very close to those obtained through more sophisticated calculations.[28,48,49] The orientational dynamics is then incorporated through $\Gamma_R(k,z)$, which is, in turn, connected to the experimentally measured frequency dependent dielectric function, $\varepsilon(z)$, by[32−36]

$$\frac{2k_BT}{I[z + \Gamma_R(k,z)]} = \frac{z\varepsilon_0[\varepsilon(z) - \varepsilon_\infty]}{f(110;k=0)\varepsilon_\infty[\varepsilon_0 - \varepsilon(z)]} \quad (5)$$

where ε_∞ is the dielectric constant in the high-frequency limit and I is the moment of inertia. $f(110,k)$ is related to the orientational direct correlation function, $c(110,k)$, through the relation[45,46] $f(110,k) = 1 - (\rho_d^0/4\pi)c(110,k)$.

The temperature-dependent dielectric relaxation data used in the present calculation are those obtained in measurements[28] spanning a wide range of frequencies ($0.2 \le \nu/\mathrm{GHz} \le 89$) and a temperature range of $278.15 \le T/\mathrm{K} \le 338.15$. In the study from which these data were obtained, $\varepsilon(z)$ was found to fit the following form at all temperatures

$$\varepsilon(z) = \varepsilon_\infty + \frac{S_1}{[1 + (z\tau_1)^{1-\alpha_1}]^{\beta_1}} + \frac{S_2}{(1 + z\tau_2)} \quad (6)$$

where τ_j denotes the relaxation time associated with the S_j dispersion. The parameters α_1 and β_1 determine the shape of a relaxation spectrum. For the sake of completeness, the experimental dielectric relaxation data, which are also required for interpreting the calculated results, are provided in Table 1.

The isotropic liquid dynamic structure factor is related to the translational frictional kernel $[\Gamma_T(k,z)]$ as[32]

$$\frac{k_BT}{M\sigma^2[z + \Gamma_T(k,z)]} = \frac{S(k)[S(k) - zS(k,z)]}{k^2S(k,z)} \quad (7)$$

with $S(k,z) = S(k)/[z + D_Tk^2/S(k)]$, where the translational diffusion coefficient D_T was obtained from the experimental viscosity and slip boundary condition using the effective volume of an ionic liquid molecule. The static isotropic structure factor was approximated by that for Percus−Yevick hard spheres.[50] Subsequently, Laplace inversion (L^{-1}) transformed the frequency-dependent quantity into a time-dependent one: $S^{lm}_{solvent}(k,t) = L^{-1}[S^{lm}_{solvent}(k,z)]$.

Note that, in eq 4, the denominator represents the square of the excess energy due to the interaction between the environment and the excited solute immediately after photoexcitation (that is, at $t = 0$). This then relaxes with time through the reorganization of the environment. The reorganization is supposed to be complete within the lifetime of the probe in its excited state. This is akin to a situation where the laser excitation induces a dipole moment in a nonpolar solute dissolved in a polar solvent and, subsequently, the created dipole drives the solvent molecules to rearrange around the excited solute until a minimum in the free energy of the (excited solute + solvent) system is attained. This energy can be identified as the dipole−dipole (solute−solvent) interaction contribution to the total dynamic Stokes shift. However, the Stokes shift in experiments is determined by the difference in interaction of the environment with the solute in its ground and excited states.[37] Therefore, $[\langle|\Delta E_{sd}(0)|^2\rangle]^{1/2}$ represents the dipole−dipole interaction contribution to the shift for a solute that becomes dipolar upon excitation. However, within the weak solute−solvent coupling limit, where solvent structural modification due to either the presence of the solute or the sudden creation of a dipole moment

TABLE 1: Temperature-Dependent Viscosities and Dielectric Relaxation Parameters Used in the Calculations[a,b]

temp (K)	viscosity (P)	ε_0	S_1	τ_1 (ps)	α_1	β_1	S_2	τ_2 (ps)	ε_∞
				[bmim][PF_6]					
288.15	5.737	16.7	12.8	2625	0.61	1	1.32	0.50	2.55
298.15	2.496	16.1	12.0	1178	0.57	1	1.86	0.47	2.24
308.15	1.401	17.2	13.2	905	0.58	1	1.61	0.48	2.30
318.15	0.811	16.8	12.9	535	0.56	1	1.39	0.64	2.56
328.15	0.531	13.9	9.8	166	0.50	1	1.71	0.61	2.39
338.15	0.358	13.0	8.5	106	0.43	1	1.23	1.39	3.27
				[bmim][BF_4]					
278.15	3.192	14.4	10.1	670	0.59	1	3.24	0.26	1.10
288.15	1.947	14.1	9.64	351	0.54	1	2.78	0.40	1.72
298.15	0.996	14.6	10.0	284	0.52	1	2.04	0.62	2.57
308.15	0.582	13.8	9.09	140	0.49	1	1.68	0.80	2.98
318.15	0.378	13.3	8.43	93.7	0.45	1	1.71	0.94	3.11
328.15	0.290	12.5	7.56	59.4	0.40	1	1.76	0.97	3.17
338.15	0.208	12.5	7.34	52.5	0.39	1	1.58	1.42	3.56
				[bmim][DCA]					
278.15	0.660	12.4	7.93	150	0.43	1	1.20	0.73	3.24
288.15	0.434	11.7	7.14	89.3	0.39	1	1.12	1.06	3.48
298.15	0.293	11.3	6.42	63.0	0.33	1	0.75	2.09	4.11
308.15	0.203	11.0	6.04	49.1	0.30	1	1.41	1.39	3.58
318.15	0.144	11.1	6.24	41.4	0.32	1	1.47	1.25	3.42
328.15	0.104	10.8	5.75	34.6	0.29	1	1.66	1.32	3.40
338.15	0.077	11.0	6.14	28.9	0.32	1	1.46	1.21	3.36
				[hmim][BF_4]					
278.15	5.750	11.0	7.03	1048	0.60	1	1.33	0.50	2.68
288.15	3.157	12.3	8.27	893	0.58	1	1.52	0.50	2.51
298.15	1.741	12.0	7.87	451	0.54	1	1.95	0.44	2.18
308.15	1.030	12.2	8.09	283	0.53	1	1.91	0.46	2.20
318.15	0.659	12.8	8.70	240	0.52	1	1.63	0.58	2.49
328.15	0.445	12.5	8.47	151	0.50	1	2.14	0.44	1.93
338.15	0.339	12.6	8.29	121	0.48	1	1.22	0.98	3.06
				[emim][BF_4]					
278.15	0.761	16.3	11.0	99.3	0.46	1	1.85	1.00	3.41
288.15	0.532	15.6	10.2	60.7	0.44	1	1.65	1.26	3.69
298.15	0.372	14.5	8.70	46.6	0.36	1	2.05	1.22	3.75
308.15	0.256	13.6	7.42	36.6	0.31	1	2.13	1.60	4.07
318.15	0.188	13.0	7.31	21.9	0.34	1	1.91	1.30	3.75
328.15	0.127	12.6	6.51	18.4	0.26	1	2.41	1.24	3.64
338.15	0.089	12.1	5.84	15.5	0.20	1	2.48	1.29	3.79
				[emim][DCA]					
278.15	0.403	11.7	5.95	46.4	0.23	1	1.49	1.88	4.30
288.15	0.288	11.3	5.28	34.5	0.18	1	1.69	2.14	4.37
298.15	0.210	11.0	4.97	30.7	0.16	1	1.90	1.84	4.18
308.15	0.156	10.5	4.25	25.2	0.13	1	1.95	2.08	4.33
318.15	0.119	10.0	3.55	18.9	0.08	1	2.11	2.11	4.31
328.15	0.091	10.1	3.74	16.7	0.10	1	2.06	2.11	4.32
338.15	0.072	10.0	3.17	16.1	0.03	1	2.38	2.49	4.42
				[hmim][NTf_2]					
278.15	2.141	13.8	10.6	925	0.55	1	0.43	0.80	2.77
288.15	1.146	12.1	8.72	299	0.47	1	0.65	0.80	2.71
298.15	0.678	12.7	9.40	233	0.47	1	0.68	0.80	2.58
308.15	0.433	11.6	8.11	128	0.40	1	1.09	0.69	2.40
318.15	0.294	11.9	8.40	107	0.39	1	0.97	0.80	2.52
328.15	0.210	11.3	7.68	73.1	0.34	1	1.19	0.80	2.38
338.15	0.157	11.2	7.56	64.0	0.33	1	1.03	1.2	2.66

[a] Experimentally measured dielectric relaxation parameters were taken from ref 28. [b] Viscosities were taken from references: Ref 39. Gu, Z.; Brennecke, J. F. *J. Chem. Eng. Data* **2002**, *47*, 339. Zhou, Q.; Wang, L. S.; Chen, H. P. *J. Chem. Eng. Data* **2006**, *51*, 905. Fredlake, C. P.; Crosthwaite, J. M.; Hert, D. G.; Aki, S. N. V. K.; Brennecke, J. F. *J. Chem. Eng. Data* **2004**, *49*, 954. Yoshida, Y.; Baba, O.; Saito, G. *J. Phys. Chem. B* **2007**, *111*, 4742. Sanmamed, Y. A.; Gonzalez-Salgado, D.; Troncoso, J.; Cerdeirina, C. A.; Romani, L. *Fluid Phase Equilib.* **2007**, *252*, 96. Navia, P.; Troncoso, J.; Romani, L. *J. Chem. Eng. Data* **2007**, *52*, 1369. Taguchi, R.; Machida, H.; Sato, Y.; Smith, R. L., Jr. *J. Chem. Eng. Data* **2009**, *54*, 22. Zhang, S.; Li, X.; Chen, H.; Wang, J.; Zhang, J.; Zhang, M. *J. Chem. Eng. Data* **2004**, *49*, 760. Leong, T. I.; Sun, I. W.; Deng, M. J.; Wu, C. M.; Chen, P. Y. *J. Electrochem. Soc.* **2008**, *155*, F55-560. Tokuda, H.; Hayamizu, K.; Ishii, K.; Susan, Md. A. B. H.; Watanabe, M. *J. Phys. Chem. B* **2005**, *109*, 6103. Note that some data were interpolated or extrapolated wherever necessary.

in it can be assumed to be negligible, $[\langle|\Delta E_{sd}(0)|^2\rangle]^{1/2}$ should provide a reasonably good description for the dipolar contribution to the observed shift.

C. Calculation of the Solute−Solvent Ion−Dipole Interaction Contribution, $S_{si}(t)$. The expression for the normalized dipole−ion solvation energy autocorrelation function can be written as[30]

$$S_{si}(t) = \frac{\langle \Delta E_{si}(t)\, \Delta E_{si}(0)\rangle}{\langle |\Delta E_{si}(0)|^2\rangle} = \frac{2\left(\frac{k_B T}{2\pi}\right)^2 \sum_{\alpha,\beta} \sqrt{n_\alpha^0 n_\beta^0} \int_0^\infty dk\, k^2 S_{solute}^{10}(k;t)\, c_{s\alpha}^{10}(k)\, c_{s\beta}^{10}(-k)\, S_{\alpha\beta}^{ion}(k;t)}{2\left(\frac{k_B T}{2\pi}\right)^2 \sum_{\alpha,\beta} \sqrt{n_\alpha^0 n_\beta^0} \int_0^\infty dk\, k^2 S_{solute}^{10}(k)\, c_{s\alpha}^{10}(k)\, c_{s\beta}^{10}(-k)\, S_{\alpha\beta}^{ion}(k)} \tag{8}$$

Note that a detailed derivation of eq 8 has already been provided in ref 30 and thus is not elaborated here. $S_{\alpha\beta}^{ion}(k,t)$ is the isotropic ion dynamic structure factor and can be obtained through the Laplace inversion, $S_{\alpha\beta}^{ion}(k,t) = L^{-1}[S_{\alpha\beta}^{ion}(k,z)]$.

The wavevector- and frequency-dependent isotropic ion dynamic structure factor $[S_{\alpha\beta}^{ion}(k,z)]$ is related to the translational frictional kernel $[\Gamma_T^{ion}(k,z)]$ as[30,51]

$$\frac{k_B T}{M\sigma^2[z + \Gamma_T^{ion}(k,z)]} = \frac{S_{\alpha\beta}^{ion}(k)[S_{\alpha\beta}^{ion}(k) - zS_{\alpha\beta}^{ion}(k,z)]}{k^2 S_{\alpha\beta}^{ion}(k,z)} \tag{9}$$

where M denotes the mass and σ is the hard-sphere diameter of the translating ion. $S_{\alpha\beta}^{ion}(k,z)$ is approximated by its diffusive limit[30,51]

$$S_{\alpha\beta}^{ion}(k,z) = \frac{S_{\alpha\beta}^{ion}(k)}{z + D_T^{ion} k^2 / S_{\alpha\alpha}^{ion}(k)} \tag{10}$$

where the translational diffusion coefficient of an ion (D_T^{ion}) was obtained from the experimental viscosity and slip boundary condition using the hard-sphere radius of the moving ion. The isotropic static ion structure factor, $S_{\alpha\beta}^{ion}(k)$, was calculated using the relation[52,53]

$$S_{\alpha\beta}^{ion}(k) = \delta_{\alpha\beta} - \frac{4\pi\sqrt{n_\alpha^0 n_\beta^0} q_\alpha q_\beta}{k_B T \varepsilon_0 (1 + k\sigma)} \frac{\kappa^2}{\kappa_D{}^2} \frac{\cos(k\sigma) + \frac{\kappa}{k}\sin(k\sigma)}{(k^2 + \kappa^2)} \tag{11}$$

where q_α is the charge of the αth type of ion and κ is the renormalized screening constant. κ is related to the Debye screening constant, κ_D, as

$$\kappa = \frac{\kappa_D}{\sqrt{1 - (\kappa_D\sigma)^2/2 + (\kappa_D\sigma)^3/6}} \tag{12}$$

with

$$\kappa_D = \sqrt{\frac{4\pi}{k_B T \varepsilon_0} \sum_\alpha n_\alpha^0 q_\alpha{}^2}$$

TABLE 2: Parameters Used to Calculate Static Structure Factors

		molecular weight (g/mol)		ionic radius[a] (Å)		
ionic liquid	dipole moment[b] (D)	cation	anion	cation	anion	density[c] (g/cm^3)
[bmim][PF_6]	4.4	139.2	145.0	3.39	2.72	1.377 (288.15), 1.368 (298.15), 1.360 (308.15), 1.349 (318.15), 1.339 (328.15), 1.329 (338.15)
[bmim][BF_4]	3.7	139.2	86.8	3.39	2.29	1.217 (278.15), 1.209 (288.15), 1.202 (298.15), 1.195 (308.15), 1.189 (318.15), 1.183 (328.15), 1.177 (338.15)
[bmim][DCA]	3.8	139.2	66.0	3.39	2.50	1.062 (278.15), 1.059 (288.15), 1.057 (298.15), 1.055 (308.15), 1.050 (318.15), 1.044 (328.15), 1.038 (338.15)
[hmim][BF_4]	3.9	167.3	86.8	3.57	2.29	1.159 (278.15), 1.152 (288.15), 1.145 (298.15), 1.138 (308.15), 1.131 (318.15), 1.124 (328.15), 1.117 (338.15)
[emim][BF_4]	3.7	113.2	86.8	3.03	2.29	1.295 (278.15), 1.288 (288.15), 1.279 (298.15), 1.272 (308.15), 1.265 (318.15), 1.258 (328.15), 1.250 (338.15)
[emim][DCA]	3.4	113.2	66.0	3.03	2.50	1.098 (278.15), 1.082 (288.15), 1.066 (298.15), 1.050 (308.15), 1.034 (318.15), 1.018 (328.15), 1.002 (338.15)
[hmim][NTf_2]	5.0	167.3	280.1	3.57	3.39	1.386 (278.15), 1.376 (288.15), 1.366 (298.15), 1.356 (308.15), 1.345 (318.15), 1.335 (328.15), 1.325 (338.15)

[a] From references: Tokuda, H.; Hayamizu, K.; Ishii, K.; Susan, Md. A. B. H.; Watanabe, M. *J. Phys. Chem. B* **2005**, *109*, 6103. Tokuda, H.; Ishii, K.; Susan, Md. A. B. H.; Tsuzuki, S.; Hayamizu, K.; Watanabe, M. *J. Phys. Chem. B* **2006**, *110*, 2833. Ref 14. Ref 48. [b] Dipole moments of the effective dipolar liquids calculated from the MSA using the experimental dielectric constant at 298.15 K, assumed to be the same for all temperatures. [c] From references: Ref 39. Gu, Z.; Brennecke, J. F. *J. Chem. Eng. Data* **2002**, *47*, 339. Zhou, Q.; Wang, L. S.; Chen, H. P. *J. Chem. Eng. Data* **2006**, *51*, 905. Fredlake, C. P.; Crosthwaite, J. M.; Hert, D. G.; Aki, S. N. V. K.; Brennecke, J. F. *J. Chem. Eng. Data* **2004**, *49*, 954. Yoshida, Y.; Baba, O.; Saito, G. *J. Phys. Chem. B* **2007**, *111*, 4742. Sanmamed, Y. A.; Gonzalez-Salgado, D.; Troncoso, J.; Cerdeirina, C. A.; Romani, L. *Fluid Phase Equilib.* **2007**, *252*, 96. Navia, P.; Troncoso, J.; Romani, L. *J. Chem. Eng. Data* **2007**, *52*, 1369. Taguchi, R.; Machida, H.; Sato, Y.; Smith, R. L., Jr. *J. Chem. Eng. Data* **2009**, *54*, 22. Zhang, S.; Li, X.; Chen, H.; Wang, J.; Zhang, J.; Zhang, M. *J. Chem. Eng. Data* **2004**, *49*, 760. Leong, T. I.; Sun, I. W.; Deng, M. J.; Wu, C. M.; Chen, P. Y. *J. Electrochem. Soc.* **2008**, *155*, F55-560. Tokuda, H.; Hayamizu, K.; Ishii, K.; Susan, Md. A. B. H.; Watanabe, M. *J. Phys. Chem. B* **2005**, *109*, 6103. Note that some data were obtained from interpolation or extrapolation wherever necessary.

$\delta_{\alpha\beta}$ signifies the Kronecker's delta representation, which means that $\delta_{\alpha\beta} = 1$ if the correlation is considered between ions of the same type (cation or anion) and $\delta_{\alpha\beta} = 0$ otherwise. Table 2 summarizes the parameters required for the calculations of the static structure factors. The solute dynamic structure factor, $S^{lm}_{solute}(k,t)$ is assumed to be given by[45] $S^{lm}_{solute}(k,t) = (1/4\pi) \exp\{-[l(l+1)D^s_R + k^2 D^s_T]t\}$. The rotational ($D^s_R$) and translational ($D^s_T$) diffusion coefficients of the solute were obtained from experimental viscosity using respectively the stick-and-slip hydrodynamic boundary conditions.[50]

D. Calculation of the Wavevector-Dependent Direct Correlation Function between Ions and the Dipolar Solute, $c^{10}_{s\alpha}(k)$. The longitudinal component of the wavevector-dependent direct correlation function between the dipolar solute and ions, $c^{10}_{s\alpha}(k)$, was again approximated as that in the homogeneous limit and was taken as[32,45]

$$c^{10}_{s\alpha}(k) = -\sqrt{\frac{4\pi}{3}}\left(\frac{4\pi i \mu_1 q_\alpha}{k_B T \varepsilon_0 k}\right)\frac{\sin(kr_c)}{kr_c} \qquad (13)$$

where μ_1 is the dipole moment of the excited solute and r_c is the distance of the closest approach between the solute and a given ionic species.

Equation 8 indicates that the center-of-mass motion of the ions is responsible for the relaxation of the solute−ion (dipole−ion) interaction contribution. This involves structural relaxation of the ion dynamic structure factor and induces a red shift in the fluorescence spectrum on the translational diffusion time scale. Because the diffusion time scale is associated with molecular-length-scale processes (involving nearest neighbors),[45] the effects on the spectrum arise after the orientational polarization relaxation is complete. The details of the solvent structure around the solute become more relevant at this time scale, as breakage and formation of the solvation shell occur through translational motion of the solvating species.[54] Consequently, static heterogeneity, if present, assumes more importance after the initial phase of solvation energy relaxation. Because the heterogeneity of any type (spatial or temporal) is completely neglected in the present theory, the calculated results are expected to describe only the qualitative features of the experimental dynamics. However, the dominance of the collective ($k\sigma \rightarrow 0$) solvent modes in the Stokes shift dynamics of dipolar ionic liquids[29] has considerably reduced the importance of the detailed solvent structure, leading to a much better agreement than expected. According to the present theory, it is this center-of-mass motion of ions that produces the slow long-time tail of the observed dynamics in ionic liquids and electrolyte solutions.

The above discussion suggests that the ion−solute contribution to the dynamical Stokes shift can be approximated as $[\langle|\Delta E_{si}(0)|^2\rangle]^{1/2}$, which can be calculated easily from the denominator of eq 8. The calculated total dynamic Stokes shift is then expressed as[30]

$$\Delta\nu^t = \Delta\nu^t_{sd} + \Delta\nu^t_{si} = \sqrt{\langle|\Delta E_{sd}(0)|^2\rangle} + \sqrt{\langle|\Delta E_{si}(0)|^2\rangle} \qquad (14)$$

The calculated shifts reported here were obtained using eq 14. Densities, viscosities, and diffusion coefficients required in the

calculation were taken from the literature and interpolated and extrapolated wherever necessary. The excited-state dipole moment of C153 was taken to be 14 D at all temperatures.[37,55] The temperature dependence enters into the present calculation through the (i) prefactors, (ii) the solute−solvent dipole−dipole and dipole−ion direct correlation functions, (iii) the orientational and isotropic (translational) dynamic structure factors of the dipolar ionic species, (iv) the translational dynamic structure factor of the ions, and (v) the solute dynamic structure factor. The present theory therefore not only enables the prediction of the overall temperature dependence of the Stokes shift and its dynamics in these ionic liquids but also reveals the microscopic origin of the observed dependence, as each of the contributing components can be separately analyzed.

III. Numerical Results

A. Calculated Dynamic Stokes Shift: Temperature Dependence. We now present the calculated temperature-dependent dynamic Stokes shift for C153 in seven different imidazolium ionic liquids: [bmim][PF_6], [bmim][BF_4], [bmim][DCA], [emim][BF_4], [emim][DCA], [hmim][BF_4], and [hmim][NTf_2]. The calculated total dynamic Stokes shifts ($\Delta\nu^t$), along with the solute−solvent dipole−dipole ($\Delta\nu^t_{sd}$) and dipole−ion ($\Delta\nu^t_{si}$) interaction contributions, for the temperature range of 278.15 $\leq T/K \leq$ 338.15 are summarized in Table 3 where the slope of the calculated dependence, $d\Delta\nu^t/dT$, is also shown in the last column. The following general observations can be made immediately from this table: (i) the calculated total shift ranges roughly between ∼1600 and ∼2500 cm^{-1} for these ionic liquids in the above temperature range; (ii) the dipole−ion (solute−ion) interaction ($\Delta\nu^t_{si}$) constitutes approximately 50−60% of the total calculated shift ($\Delta\nu^t$); (iii) the total change in calculated $\Delta\nu^t$ values is rather small (only 10−20% in a given liquid) and in the range of ∼200−400 cm^{-1}; (iv) the increase in solution temperature increases $\Delta\nu^t$, except for [hmim][BF_4], for which the calculated total shift decreases with increase in temperature; (v) the increase in dipole−dipole interaction contribution ($\Delta\nu^t_{sd}$) with temperature for all of these ionic liquids is ∼2% (between ∼20−50 cm^{-1}); and (vi) the enhancement of the dipole−ion contribution is ∼25% and thus much larger (130 $\leq \Delta\nu^t_{si}/cm^{-1} \leq$ 335), except for [hmim][BF_4], for which $\Delta\nu^t_{si}$ decreases with temperature. Note that, whereas the first two observations are in agreement with the existing experimental data[56] and our earlier theoretical study for a few imidazolium ionic liquids at room temperature,[30] the rest of the predictions are completely new and thus require comparison with experimental data to test the validity of the present theory.

Recently, dynamic Stokes shifts of C153 in a few ammonium and pyrrolidinium ionic liquids with a common anion, $[NTf_2]^-$, were measured[24] in nearly the same temperature range as considered here. The measured dynamic Stokes shifts were found to vary between ∼1300 and 1600 cm^{-1} for the ammonium ionic liquids and between ∼1000 and 1500 cm^{-1} for the pyrrolidinium analogues, although a certain portion of the total shift is believed to have been missed, particularly at high temperature and low viscosity, because of the limited time resolution (∼10 ps) employed in those experiments.[24] The measured shifts for the relatively more viscous ammonium ionic liquids were found to increase with temperature. Moreover, the measured temperature-induced total change in $\Delta\nu^t$ for these liquids is ∼200−400 cm^{-1}, which is strikingly similar to the prediction for the imidazolium ionic liquids considered here. The similarity in the temperature-induced total changes of $\Delta\nu^t$ for ammonium and imidazolium ionic liquids might initially appear surprising. However, if the prediction that the temperature dependence of the total shift is mainly that of the dipole−ion contribution ($\Delta\nu^t_{si}$) is considered together with the result that $\Delta\nu^t_{si}$ constitutes more than half of the total shift for imidazolium ionic liquids (see Table 3 and ref 30) and almost the entire shift for nondipolar ionic liquids,[30] then a very similar temperature dependence of the dynamic Stokes shift in all of these ionic liquids should be expected. Temperature-dependent (253 $\leq T/K \leq$ 333) dynamic Stokes shift measurements for the charge-transfer (CT) band of 9,9′-bianthryl (BA) in several imidazolium ionic liquids containing $[BF_4]^-$, $[PF_6]^-$, or trifluoromethylsulfonyl imide ($[TFSI]^-$) anion, on the other hand, indicated[23] a total shift that varies approximately between ∼1300 and 2800

TABLE 3: Temperature-Dependent Dynamic Stokes Shift ($\Delta\nu^t$)

temperature (K)	dipole−dipole contribution, $\Delta\nu^t_{sd}$ (cm^{-1})	ion−dipole contribution, $\Delta\nu^t_{si}$ (cm^{-1})	total ($\Delta\nu^t = \Delta\nu^t_{sd} + \Delta\nu^t_{si}$)($cm^{-1}$)	$d(\Delta\nu^t)/dT$ (cm^{-1}/K)
		C153 in [bmim][PF_6]		
288.15	864	849	1713	5.03
298.15	871	877	1748	
308.15	876	812	1688	
318.15	882	827	1709	
328.15	889	1007	1896	
338.15	896	1076	1972	
		C153 in [bmim][BF_4]		
278.15	831	1054	1885	3.36
288.15	845	1071	1916	
298.15	853	1026	1879	
308.15	860	1084	1944	
318.15	866	1122	1988	
328.15	872	1193	2065	
338.15	877	1186	2063	
		C153 in [bmim][DCA]		
278.15	826	1212	2038	2.64
288.15	833	1285	2118	
298.15	839	1330	2169	
308.15	845	1363	2208	
318.15	850	1344	2194	
328.15	855	1376	2231	
338.15	859	1342	2201	
		C153 in [hmim][BF_4]		
278.15	799	1285	2084	−2.48
288.15	804	1134	1938	
298.15	809	1157	1966	
308.15	813	1130	1943	
318.15	818	1067	1885	
328.15	821	1088	1909	
338.15	827	1072	1899	
		C153 in [emim][BF_4]		
278.15	910	1014	1924	6.45
288.15	918	1057	1975	
298.15	926	1136	2062	
308.15	933	1210	2143	
318.15	939	1263	2202	
328.15	945	1299	2244	
338.15	951	1349	2300	
		C153 in [emim][DCA]		
278.15	851	1409	2260	3.16
288.15	855	1446	2301	
298.15	858	1473	2331	
308.15	861	1531	2392	
318.15	864	1595	2459	
328.15	866	1561	2427	
338.15	868	1560	2428	
		C153 in [hmim][NTf_2]		
278.15	763	817	1580	2.7
288.15	769	935	1704	
298.15	773	882	1655	
308.15	777	965	1742	
318.15	781	933	1714	
328.15	785	980	1765	
338.15	788	983	1771	

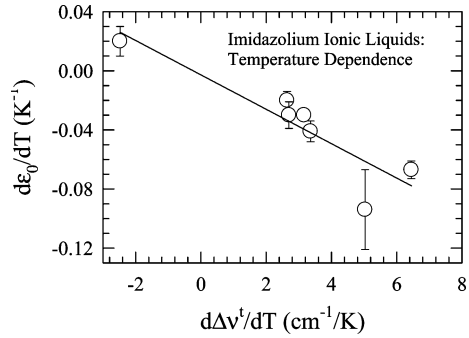

Figure 1. Correlation between the temperature coefficients of the measured static dielectric constant and the calculated total dynamic Stokes shift for the imidazolium ionic liquids considered. The circles with error bars denote values for these ionic liquids, and the line denotes a linear regression fit through these symbols with a correlation coefficient (R) of 0.9.

cm^{-1}. This is also in qualitative agreement with the results predicted here. In addition, these measurements[23] reveal a slope of nearly 6 cm^{-1}/K for the temperature dependence of the asymptotic CT band peak obtained from the time-resolved experiments [that is, $\nu_{CT}(t = \infty)$] with BA in [bmim][TFSI] and [emim][TFSI]. Similar analyses using the data for C153 in ammonium and pyrrolidinium ionic liquids[24] produce a slope of ~1 cm^{-1}/K. The slopes, $d\Delta\nu^t/dT$, obtained in the present work and summarized in Table 3 for C153 in various imidazolium ionic liquids ([hmim][BF$_4$] being an exception) are therefore well within this range, suggesting the validity of the present calculation scheme for studying the temperature dependence of Stokes shift dynamics in these ionic liquids.

Next, we explore whether the ionic liquid [hmim][BF$_4$] is really very different from other liquids considered here, as well as the correlation between the slopes ($d\varepsilon_0/dT$) obtained from temperature-dependent dielectric relaxation measurements of these liquids[28] and those ($d\Delta\nu^t/dT$) from the calculated temperature-dependent total dynamic Stokes shifts. Figure 1 depicts such a correlation, where these slopes exhibit an inverse linear relationship. Note that the $d\varepsilon_0/dT$ values for these ionic liquids are very low[28] and range between 0.04 and −0.10. This suggests that the rise in temperature does not significantly disturb the long-wavelength static orientational correlations in these ionic liquids.[47,50] In addition, the temperature dependence of the solvent dipole moment for these ionic liquids also becomes weak as the former is calculated from measured ε_0 values. Because these static orientational correlations (both solute−solvent and solvent−solvent) at the long-wavelength ($k\sigma \rightarrow 0$) limit govern the magnitude of the Stokes shift in the present theory, the predicted overall weak temperature dependence of the Stokes shift for these liquids is expected. The temperature dependence of the dipole−dipole contribution ($\Delta\nu^t_{sd}$) is insignificant (~2%) because of negligible changes in these static dipole−dipole correlations and the solvent dipole moment. However, for $\Delta\nu^t_{si}$, the temperature dependence is relatively stronger because the solute−solvent ion−dipole static correlation, which is very large in the $k\sigma \rightarrow 0$ limit (see eq 13), varies inversely as ε_0. In fact, $(1/\varepsilon_0)^2$ increases by ~25−40% in these liquids as the temperature is changed in this range. As a result, $\Delta\nu^t_{si}$ changes approximately by the same amount. The increase in $\Delta\nu^t_{si}$ with temperature can be interpreted as arising out of the enhanced solute−ion (dipole−ion) interaction due to the decrease in ε_0 with temperature for these ionic liquids. This also explains why $d\varepsilon_0/dT$ for [hmim][BF$_4$] is positive but $d\Delta\nu^t/dT$ is negative. It is therefore natural that [hmim][BF$_4$], which appeared to be

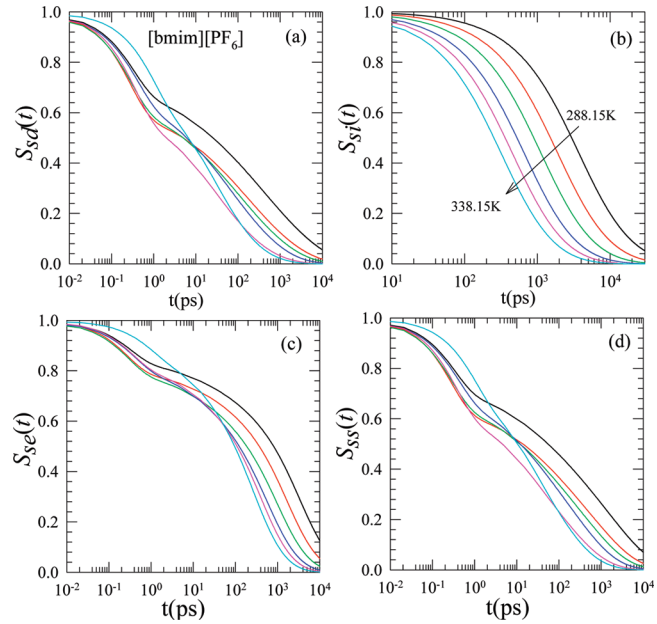

Figure 2. Temperature dependence of the calculated solvation response function for C153 in [bmim][PF$_6$]. The four different panels describe the temperature dependence of different predicted contributions: (a) solute−solvent dipole−dipole interaction part, $S_{sd}(t)$, using eq 4; (b) solute−solvent dipole−ion interaction part, $S_{si}(t)$, using eq 8; (c) total, $S_E(t)$, using eq 3; (d) constructed, $S_{ss}(t) = 0.90S_{sd}(t) + 0.10S_{si}(t)$. The black, red, green, blue, magenta, and cyan lines represent the calculated response functions at 288.15, 298.15, 308.15, 318.15, 328.15, and 338.15 K, respectively. Note that the subpicosecond component originates only through the $S_{sd}(t)$ component. The Laplace inversion discussed in the text was performed by using the Stehfest algorithm (Stehfest, H. Commun. ACM 1970, 13, 624.).

different from the other ionic liquids in both the dielectric relaxation measurements (positive slope) and the Stokes shift calculations (negative slope), obeys the same correlation as the others. Interestingly, thermosolvatochromic studies with pyridinium, pyrrolidinium, and imidazolium ionic liquids have also indicated a decrease in solution polarity [more specifically, the $E_T(30)$ values] with increasing temperature.[57−60] Because the present theory suggests enhanced solute−solvent interaction due to a decrease in ε_0 when the temperature is raised, a red shift in the spectrum (absorption or emission) of dye molecule dissolved in these liquids is expected. This then naturally leads to lowering of the $E_T(30)$ value, as it is inversely proportional to λ_{max}, where the latter denotes the wavelength corresponding to the absorption maximum for Reichardt's dye[61] in these ionic liquids.

Apart from the features discussed above, there still remain a few subtle aspects of the calculated shifts that warrant further discussion. For example, the calculated temperature-dependent total shift is the largest among all at any given temperature for [emim][DCA] (ranges between 2260 and 2430 cm^{-1}) and the smallest for [hmim][NTf$_2$] (ranges between 1580 and 1780 cm^{-1}). This is a reflection of the dependence of the Stokes shift on the solute−solvent size ratio,[62] the effective volume[28] (V_{eff}) being the smallest for [emim][DCA] and the largest for [hmim][NTf$_2$]. This is further supported by the calculations that both $\Delta\nu^t_{sd}$ and $\Delta\nu^t_{si}$ are uniformly larger in [emim][BF$_4$] (V_{eff} = 0.81 Å^3) than in [bmim][PF$_6$] (V_{eff} = 5.3 Å^3), even though the ε_0 values for these two liquids are comparable at these temperatures.

B. Stokes Shift Dynamics: Temperature Dependence. Next we present numerical results on the temperature-dependent Stokes shift dynamics of C153 in these seven imidazolium ionic

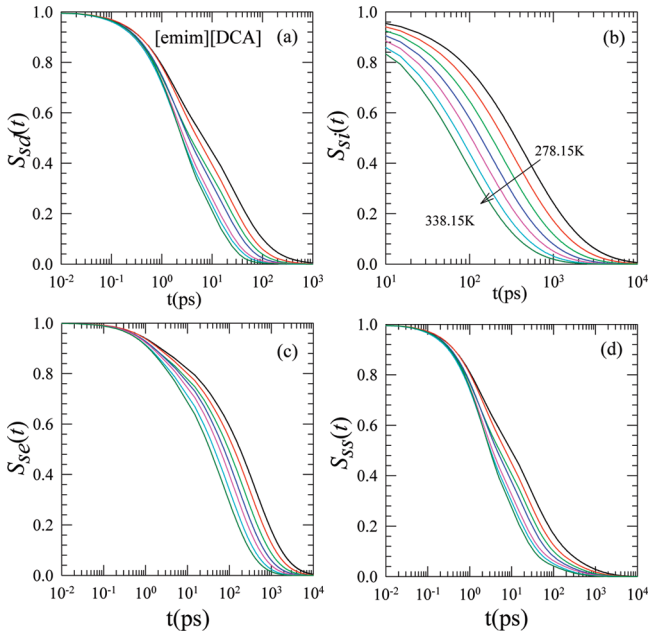

Figure 3. Temperature-dependent calculated solvation response function for C153 in [emim][DCA]. The black, red, green, blue, magenta, cyan, and dark green lines represent the calculated response functions at 278.15, 288.15, 298.15, 308.15, 318.15, 328.15, and 338.15 K, respectively. The other representations remain the same as in Figure 2.

liquids. Whereas the calculated decays of the normalized solvation energy correlation function for [bmim][PF_6] and [emim][DCA] are shown in Figures 2 and 3, the decays for five other ionic liquids are provided in the Supporting Information (Figures S1−S5). These two liquids were chosen as representative because (i) [bmim][PF_6] has the highest ε_0 value (between 17 and 13) and [emim][DCA] has the lowest (between 12 and 10) among all of the liquids at any given temperature, (ii) the effective volumes are widely different (5.3 versus 0.73 Å^3), and (iii) the viscosities span two very different ranges ($5.74 \geq \eta/P \geq 0.36$ for [bmim][PF_6] and $0.41 \geq \eta/P \geq 0.07$ for [emim][DCA]). Because all of these solvent properties are known to affect the rate of solvation energy relaxation, the difference in results can largely be attributed to the dissimilarities of these parameters.

In these Figures 2 and 3, the upper panels display the calculated decays of the normalized solvation response function due to solute−solvent dipole−dipole and dipole−ion interaction contributions [$S_{sd}(t)$ using eq 4 and $S_{si}(t)$ using eq 8, respectively], and the lower panels display the same for the total shift [$S_E(t)$, using eq 3] and a "numerically synthesized" response function, $S_{ss}(t) = 0.9S_{sd}(t) + 0.1S_{si}(t)$. The motivation for such a synthesized response function originates from our earlier works,[30] where a 10−15% contribution from $S_{si}(t)$ was found to generate almost quantitative agreement with the available experimental data for several imidazolium ionic liquids at room temperature. $S_{ss}(t)$ was therefore expected to be closer than the other three quantities to the experimental Stokes shift dynamics measured with C153 in these ionic liquids at temperatures of $278.15 \leq T/\mathrm{K} \leq 338.15$. It is evident from these figures and the related calculations shown in the Supporting Information (Figures S1−S5) that the solvation dynamics in these liquids is bimodal at these temperatures, which becomes increasingly faster as the solution temperature is raised. The decay at ∼338 K for [bmim][PF_6] does not obey this trend, which is probably due to the inaccuracy involved in the proper description of the measured dielectric relaxation spectra[28] at this temperature.

TABLE 4: Temperature Dependence of Solvation Response Function for C153 Probe in [bmim][PF_6]

type of study	a_1	τ_1 (ps)	a_2	τ_2 (ps)	β	$\langle\tau_s\rangle$ (ns)
			T = 288.15 K			
$S_{si}(t)$ (exponential)	0.65	2616	0.35	15555	1	7.14
$S_{si}(t)$ (stretched exponential)	0.38	3219	0.62	7220	0.64	7.45
$S_{sd}(t)$	0.24	0.34	0.76	453	0.31	2.76
$S_{se}(t)$	0.18	0.38	0.82	3061	0.52	4.68
$S_{ss}(t)$	0.25	0.34	0.75	891	0.35	3.36
			T = 298.15 K			
$S_{si}(t)$ (exponential)	0.68	1423	0.32	8557	1	3.70
$S_{si}(t)$ (stretched exponential)	0.39	1742	0.61	3592	0.62	3.84
$S_{sd}(t)$	0.33	0.27	0.67	205	0.33	0.86
$S_{se}(t)$	0.21	0.29	0.79	1588	0.54	2.20
$S_{ss}(t)$	0.33	0.27	0.67	428	0.37	1.20
			T = 308.15 K			
$S_{si}(t)$ (exponential)	0.68	837	0.32	4919	1	2.14
$S_{si}(t)$ (stretched exponential)	0.40	1019	0.60	2134	0.63	2.22
$S_{sd}(t)$	0.30	0.28	0.70	128	0.33	0.56
$S_{se}(t)$	0.22	0.30	0.78	866	0.52	1.26
$S_{ss}(t)$	0.31	0.28	0.69	259	0.37	0.75
			T = 318.15 K			
$S_{si}(t)$ (exponential)	0.67	485	0.33	2835	1	1.26
$S_{si}(t)$ (stretched exponential)	0.40	574	0.60	1293	0.64	1.31
$S_{sd}(t)$	0.25	0.40	0.75	81	0.34	0.34
$S_{se}(t)$	0.19	0.41	0.81	493	0.51	0.77
$S_{ss}(t)$	0.26	0.39	0.74	148	0.38	0.42
			T = 328.15 K			
$S_{si}(t)$ (exponential)	0.66	326	0.34	1894	1	0.86
$S_{si}(t)$ (stretched exponential)	0.39	379	0.61	902	0.66	0.89
$S_{sd}(t)$	0.30	0.37	0.70	40	0.35	0.14
$S_{se}(t)$	0.18	0.37	0.82	379	0.54	0.54
$S_{ss}(t)$	0.29	0.36	0.71	74	0.37	0.22
			T = 338.15 K			
$S_{si}(t)$ (exponential)	0.65	221	0.35	1279	1	0.59
$S_{si}(t)$ (stretched exponential)	0.39	263	0.61	629	0.66	0.62
$S_{sd}(t)$	0.21	1.11	0.79	42	0.42	0.10
$S_{se}(t)$	0.10	0.90	0.90	250	0.53	0.41
$S_{ss}(t)$	0.19	1.15	0.81	61	0.41	0.15

Subsequently, the calculated temperature-dependent decays for all of these liquids were fitted to a normalized function, $S^{fit}(t) = a_1 \exp(-t/\tau_1) + a_2 \exp[-(t/\tau_2)^\beta]$, to determine the amplitudes (a_i values), time constants (τ_i values), and magnitudes of the stretching exponent β associated with the calculated response functions. Note that the above equation becomes a simple biexponential function of time in the limit of $\beta = 1$. Interestingly, although $S^{fit}(t)$ was found to adequately describe $S_{si}(t)$ for both $\beta = 1$ and $0.6 < \beta < 0.7$ for all of these liquids in this temperature range, the other calculated response functions required stretched exponentials with β ranging between ∼0.3 and 0.8. Tables 4 and 5 summarize the parameters obtained from such fits to the calculated response functions and also the average solvation times, $\langle\tau_x\rangle = \int_0^\infty dt\, S_x(t)$, where x = se, sd, si, or ss, for [bmim][PF_6] and [emim][DCA], respectively. Similar fit parameters for the other liquids are provided in the Supporting Information (see Tables S6−S10).

The data in these tables clearly indicate that the solvation energy relaxation due to the solute−solvent dipolar interaction (S_{sd}) is characterized, depending on temperature and identity of the ionic liquid, by an exponentially decaying fast component

TABLE 5: Temperature Dependence of Solvation Response Function for C153 Probe in [emim][DCA]

type of study	a_1	τ_1 (ps)	a_2	τ_2 (ps)	β	$\langle\tau_s\rangle$ (ns)
			$T = 278.15$ K			
$S_{si}(t)$ (exponential)	0.63	306	0.37	1821	1	0.87
$S_{si}(t)$ (stretched exponential)	0.35	363	0.65	865	0.66	0.88
$S_{sd}(t)$	0.26	1.63	0.74	33	0.58	0.039
$S_{se}(t)$	0.06	1.76	0.94	404	0.54	0.66
$S_{ss}(t)$	0.27	3.59	0.73	52	0.43	0.10
			$T = 288.15$ K			
$S_{si}(t)$ (exponential)	0.62	210	0.38	1262	1	0.61
$S_{si}(t)$ (stretched exponential)	0.35	257	0.65	615	0.66	0.63
$S_{sd}(t)$	0.31	1.74	0.69	25	0.65	0.024
$S_{se}(t)$	0.07	2.23	0.93	294	0.55	0.46
$S_{ss}(t)$	0.32	3.26	0.68	43	0.46	0.07
			$T = 298.15$ K			
$S_{si}(t)$ (exponential)	0.60	141	0.40	870	1	0.43
$S_{si}(t)$ (stretched exponential)	0.34	187	0.66	442	0.66	0.46
$S_{sd}(t)$	0.35	1.39	0.65	21	0.68	0.018
$S_{se}(t)$	0.07	1.74	0.93	217	0.55	0.34
$S_{ss}(t)$	0.31	1.84	0.69	34	0.51	0.05
			$T = 308.15$ K			
$S_{si}(t)$ (exponential)	0.53	84	0.47	580	1	0.32
$S_{si}(t)$ (stretched exponential)	0.33	139	0.67	324	0.66	0.34
$S_{sd}(t)$	0.38	1.58	0.62	18	0.72	0.014
$S_{se}(t)$	0.07	2.31	0.93	167	0.56	0.26
$S_{ss}(t)$	0.35	2.07	0.65	30	0.55	0.03
			$T = 318.15$ K			
$S_{si}(t)$ (exponential)	0.43	41	0.57	377	1	0.23
$S_{si}(t)$ (stretched exponential)	0.32	106	0.68	243	0.66	0.25
$S_{sd}(t)$	0.43	1.58	0.57	14	0.77	0.010
$S_{se}(t)$	0.07	2.44	0.93	133	0.58	0.19
$S_{ss}(t)$	0.41	2.04	0.59	26	0.56	0.026
			$T = 328.15$ K			
$S_{si}(t)$ (exponential)	0.40	27	0.60	274	1	0.17
$S_{si}(t)$ (stretched exponential)	0.31	81	0.69	182	0.66	0.19
$S_{sd}(t)$	0.44	1.56	0.56	12	0.77	0.008
$S_{se}(t)$	0.08	2.53	0.92	102	0.58	0.15
$S_{ss}(t)$	0.43	1.92	0.57	22	0.59	0.02
			$T = 338.15$ K			
$S_{si}(t)$ (exponential)	0.40	21	0.60	215	1	0.14
$S_{si}(t)$ (stretched exponential)	0.30	64	0.70	141	0.66	0.15
$S_{sd}(t)$	0.49	1.75	0.51	11	0.84	0.007
$S_{se}(t)$	0.10	3.24	0.90	84	0.60	0.11
$S_{ss}(t)$	0.49	2.16	0.51	21	0.63	0.016

(~15−40%) with a time constant (τ_1) of nearly a picosecond or even less, followed by a relatively slower stretched exponential decay with a time constant (τ_2) spanning over approximately 10 ps to a few hundred picoseconds. It is interesting to note that, in these calculations, the ultrafast component was predicted by using the experimental dielectric relaxation parameters[28] that accounted for contributions only from the rotational processes (Cole−Cole and Debye) and not from any solvent librations. This means that fast dipolar rotation might, as observed in common polar solvents, be responsible for the subpicosecond response in the Stokes shift dynamics of these ionic liquids. The coupling of the solvent libration modes then merely accelerates further the already fast initial part of the total polar solvation energy relaxation. The decay of the solute−ion interaction part (S_{si}), on the other hand, is much slower, with both time constants being many times larger than the corresponding ones describing S_{sd}. These results and the observations made above therefore strongly suggest that the solute−solvent dipolar interaction is indeed responsible for the ultrafast component in the Stokes shift dynamics of these imidazolium ionic liquids. As expected, however, the average solvation time ($\langle\tau_s\rangle$) obtained from $S_{si}(t)$ was found to track the solution viscosity more closely, as the slow decay is linked to the relaxation of the isotropic ion dynamic structure factor. An overall increase of the stretching exponent (β) with the rise in temperature was also observed in these calculations. This indicates increased homogenization of the solvent structure at higher temperature and originates in the theory solely from the use of experimental dielectric relaxation data.

A comparative study of the predicted time constants summarized in Tables 4 and 5 seems to reveal that, although the average solvation times are uniformly shorter for [emim][DCA] than for [bmim][PF_6] because of the higher viscosity range of the latter, the fast time constant (τ_1) associated with the relaxation of the dipole−dipole interaction energy (S_{sd}) is longer by a factor of ~4−6 in the former (except at ~338 K). This is because the faster dielectric relaxation time constant for [emim][DCA] is ~3 times larger than that measured for [bmim][PF_6] at each of the temperatures studied. In addition, the relatively larger static dielectric constant of [bmim][PF_6] might also produce a steeper curvature for the free energy surface[32] in which the polar part of the solvation energy relaxes. The above results are, however, predictions of a theory that used the experimental dielectric relaxation data and, hence, was tuned to how good the different models are in accurately describing the experimental dielectric relaxation measurements. With such a caveat notwithstanding, a factor of ~4−6 difference is too large to be suggested to arise from either the inaccurate description of dielectric relaxation in these liquids or the approximations involved in the present theory. This prediction therefore should be tested against experiments.

Next, the temperature dependence of the calculated average solvation times, $\langle\tau_x\rangle$ (with x = sd, si, se, or ss) for these liquids are presented in Figure 4, where the inverse of the calculated times is shown on a logarithmic scale as a function of inverse temperature ($1/T$). The dependence shown in Figure 4 clearly indicates an exponential rise of average times with $1/T$ and an Arrhenius type of temperature dependence. Such behavior only indicates the dominance of solvent structural relaxation (both orientational and isotropic) on the average rate of solvation energy relaxation in these media. Note that these calculations consider only the diffusive solvent structural relaxation, as the pure solvent dynamics is incorporated through the experimental dielectric relaxation data of these liquids and assuming a diffusive center-of-mass motion of the solvent particles. Solvent dynamics due to collective solvent libration modes that appear in the terahertz (THz) domain was not included, as the frequency range covered in these dielectric relaxation measurements[28] is limited within the range $0.2 \leq \nu/\text{GHz} \leq 89$. Therefore, the intermolecular dynamics that occurs in the subpicosecond time scale[63] and was simulated to be temperature-dependent[64] does not contribute to the time scale found in these calculations. The effects of temperature on these average solvation times enter mainly through the temperature dependence of the diffusion times through liquid viscosity. Therefore, a proportionality relationship between these average solvation times and temperature is expected for these liquids.[26,65] The present calculations predict a decrease in $\langle\tau_{ss}\rangle$ by a factor of 8 for C153 in [bmim][PF_6] upon increasing the temperature from 298 to 338

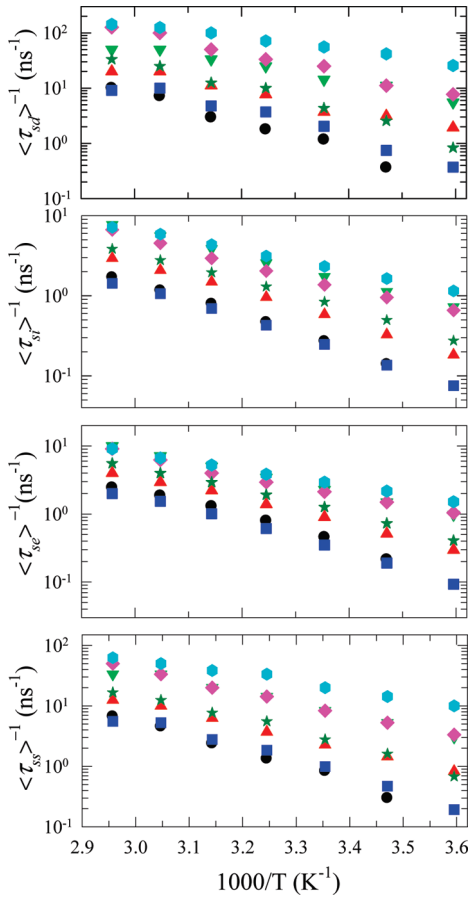

Figure 4. Temperature dependence of the calculated average solvation times for seven different imidazolium ionic liquids. Note that the calculated times (on a logarithmic scale) are shown as a function of the inverse temperature, $1/T$. The dark circles denote the ionic liquid [bmim][PF_6]; red triangles, [bmim][BF_4]; green inverted triangles, [bmim][DCA]; blue squares, [hmim][BF_4]; magenta diamonds, [emim][BF_4]; cyan hexagons, [emim][DCA]; and dark green stars, [hmim][NTf_2]. For further discussion, see the text.

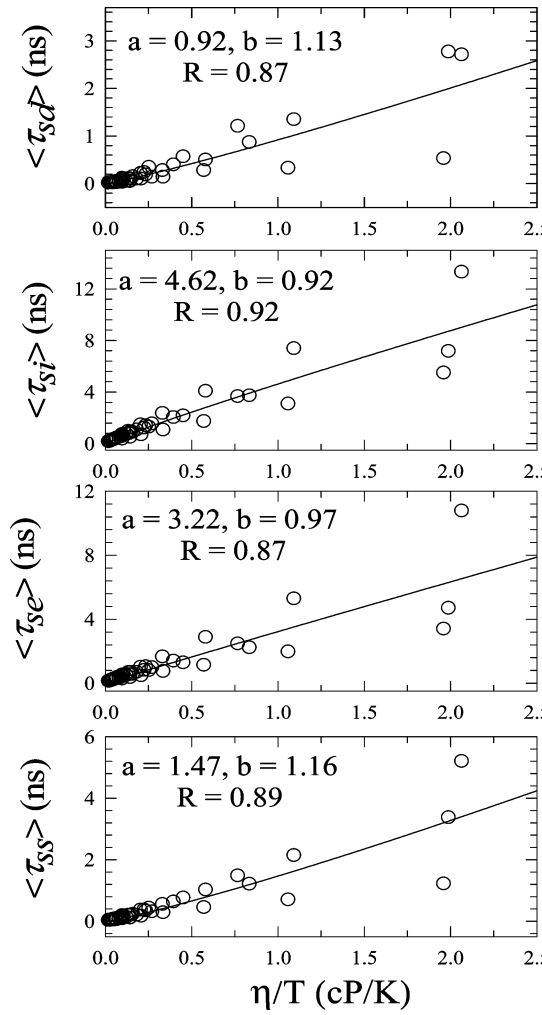

Figure 5. Viscosity dependence of the average solvation times for the imidazolium ionic liquids studied. The calculated average solvation times for various components ($\langle\tau_x\rangle$) at different temperatures are shown (circles) as a function of temperature-reduced viscosity, η/T. The line in each panel represents a fit through the calculated times (circles) of the following form: $\langle\tau_x\rangle = a(\eta/T)^b$. The fit parameters ($a$ and b) along with the corresponding value for the correlation coefficient (R) are also shown in each of the panels.

K (see Table 4). Interestingly, this is very close to earlier experimental results, where approximately an order of magnitude decrease in the measured average solvation time was observed[4] for the same liquid when the temperature was changed from 298 to 355 K. Moreover, the calculated values of $\langle\tau_{ss}\rangle$ at these two temperatures also compare well with the corresponding experimental data. These observations and those noted in the discussion of the temperature dependence of the Stokes shift, therefore, suggest that the present electrolyte solution model for these ionic liquids probably correctly includes all of the interactions that contribute to the fluorescence Stokes shift dynamics measured in time-resolved experiments. The domination of collective ($k\sigma \rightarrow 0$) solvent polarization modes in polar solvation energy relaxation[32] then substantially reduces the effects of the inappropriate modeling of solvent particles as hard spheres and the neglect of the heterogeneity of these dipolar ionic liquids.

Figure 5 shows the dependence of the calculated average solvation times, $\langle\tau_x\rangle$, on the temperature-scaled viscosity, η/T, for these ionic liquids. If the solvent motions during the stabilization of the excited probe molecule, particularly at longer times, obey the Debye−Stokes−Einstein (DSE) and Stokes−Einstein (SE) predictions,[62] then a simple power-law dependence of $\langle\tau_x\rangle$ on η/T is expected. In fact, calculated times shown in four different panels of Figure 5 do indicate such a dependence, where a fit to the theoretical results of the following form, $\langle\tau_x\rangle = a(\eta/T)^b$, produces a value for the power (b) close to unity. This is in very good agreement with what has been observed in dynamic Stokes shift measurements of many ionic liquids.[14,22,56,66]

C. Activation Energy. After the analysis of the temperature dependence of the average solvation times in Figure 4, activation energies (E_a) associated with the solvation processes in these imidazolium ionic liquids were determined. Even though a more complex form such as the Vogel−Fulcher−Tammann (VFT) equation might be more appropriate for analyzing the temperature dependence,[24] we employed the traditional Arrhenius approach to estimate the activation energy because of neglect of the static heterogeneity while calculating the static correlations in these liquids. Note that, in these liquids, particularly at low temperatures, there could be a distribution of activation energies due to domain formation,[15] and thus, the idea of a single activation energy signifying homogeneity in the environment might not be appropriate. However, an Arrhenius-type description can still be used to estimate the average activation energy, and in the present scenario, a close correlation between E_a from the calculated solvation times and that determined from the viscosity measurements is expected. Table 6 summarizes the results, where the calculated solvation times were fitted to the

TABLE 6: Arrhenius Activation Energies[a]

system	$E_a(\langle\tau_{sd}\rangle)$ (kJ mol^{-1})	$E_a(\langle\tau_{si}\rangle)$ (kJ mol^{-1})	$E_a(\langle\tau_{se}\rangle)$ (kJ mol^{-1})	$E_a(\langle\tau_{ss}\rangle)$ (kJ mol^{-1})	$E_a(\langle\kappa\rangle)$ (kJ mol^{-1})	$E_a(\langle\eta\rangle)$ (kJ mol^{-1})	$E_a(\langle\tau_1^{DR}\rangle)$ (kJ mol^{-1})
[bmim][PF_6]	52.3	40.4	39.3	49.3	38.5 ± 1.6	43.5 ± 0.1	38.4 ± 9.1
[bmim][BF_4]	33.1	36.4	34.3	36.5	33.5 ± 1.3	34.6 ± 1.2	32.0 ± 3.1
[bmim][DCA]	29.4	31.0	30.4	33.1	25.4 ± 0.8	27.4 ± 0.4	19.0 ± 1.4
[hmim][BF_4]	44.2	39.2	40.6	45.0	39.4 ± 1.1	39.2 ± 0.6	28.7 ± 1.8
[emim][BF_4]	37.7	30.2	27.8	35.4	21.5 ± 0.5	27.5 ± 0.4	24.1 ± 1.3
[emim][DCA]	22.3	24.2	22.9	24.3	16.4 ± 0.3	24.1 ± 0.7	14.4 ± 0.9
[hmim][NTf_2]	46.9	34.2	33.9	41.4	30.4 ± 1.4	31.6 ± 0.8	25.4 ± 2.6

[a] Experimental results for activation energy (E_a) for conductivity, κ; viscosity, η; and Debye relaxation time, τ_1^{DR}, taken from ref 28.

natural logarithm of the expression $\langle\tau_x\rangle = A_x \exp[E_a(x)/RT]$, where A_x denotes the pre-exponential factor and RT is the universal gas constant times the absolute temperature (T). For comparison, the activation energies obtained from the temperature-dependent measurements[28] of electrical conductivity (κ), viscosity (η) and the slowest dielectric relaxation time (τ_1^{DR}) are also listed in the same table. Note in Table 6 that activation energies obtained from conductivity and dielectric relaxation measurements are somewhat smaller than those obtained from viscosity measurements. The reason for this difference probably lies in the different degrees of coupling with the environment for these measured quantities.

Because the above-measured quantities are coupled to the same solvent−solvent interactions, the activation energies determined from them are similar. For the same reason, activation energies obtained from the calculated average solvation times for these liquids correlate well with those from the above measurements. The large values of E_a for [bmim][PF_6], [hmim][BF_4], and [hmim][NTf_2] clearly indicate a stronger dependence of the solvation energy relaxation on temperature in these liquids than in [bmim][DCA] and [emim]-[DCA]. Noticeably, the Cole−Cole parameter (α in Table 1), a sort of indicator of the degree of heterogeneity present in a liquid, is smallest for [emim][DCA] and largest for [bmim][PF_6] and [hmim][BF_4] at the lowest temperature studied.[28] Further, the E_a value obtained for [emim][DCA] from the calculated average solvation times is in very good agreement with the activation energies from the magnetic relaxation measurements of rotational motion in neat [emim] [NTf_2] (∼24 kJ mol^{-1}) and its dicyanimide analogue, [emim][$(CN)_2N$] (∼22 kJ mol^{-1}).[26] Interestingly, while the calculated activation energy for [emim]-[DCA] is very similar to that obtained from dynamic Stokes shift measurements in propanol,[67] those for [bmim][PF_6] and [hmim][BF_4] match well with the values obtained from solvation dynamics experiments involving γ-cyclodextrin aggregates[68] and aqueous micelles of Triton X-100,[69] respectively. In addition, $E_a(\langle\tau_{si}\rangle)$ and $E_a(\langle\tau_{se}\rangle)$ for [hmim][NTf_2] are quite close to the values found in time-resolved fluorescence anisotropy measurements involving the ionic liquid *N*,*N*,*N*-trimethyl-*N*-propyl ammonium bis(trifluoromethanesulfonyl) imide ([N_{3111}][NTf_2]).[70] This is expected because the solute−solvent interaction that controls the rotation of a dipolar solute in the nondipolar ionic liquid [N_{3111}][NTf_2] is the solute−ion (dipole−ion) interaction. A closer inspection of Table 6 reveals that the activation energies obtained from $\langle\tau_{sd}\rangle$ and $\langle\tau_{ss}\rangle$ are very similar to each other, and those from $\langle\tau_{si}\rangle$ and $\langle\tau_{se}\rangle$ closely follow $E_a(\eta)$ for these liquids. This correlation is shown in Figure 6. This is because of the domination of the dipole−dipole interaction contribution (S_{sd}) for $E_a(\langle\tau_{sd}\rangle)$ and $E_a(\langle\tau_{ss}\rangle)$ and ion−dipole part (S_{si}) for $E_a(\langle\tau_{si}\rangle)$ and $E_a(\langle\tau_{se}\rangle)$.

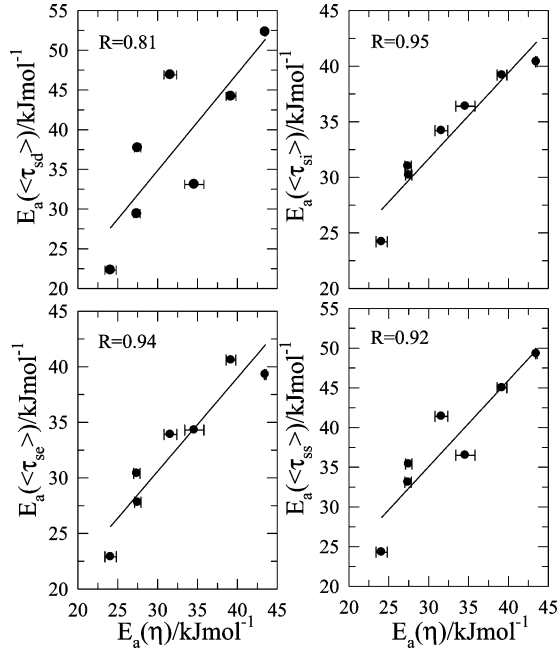

Figure 6. Correlation between the calculated activation energy for solvation, $E_a(\langle\tau_x\rangle)$ and that for viscosity, $E_a(\eta)$, determined from experiments. The lines through the points in these panels denote linear regression fits. Correlation coefficients (R) from these fits are also shown.

IV. Discussion

The present work indicates a weak dependence of the dynamic Stokes shift on temperature for the seven imidazolium ionic liquids investigated and reports an inverse correlation with the temperature dependence of the measured dielectric constant of these solvents. The decrease in static dielectric constant with temperature is predicted to increase the solute−ion static correlations, leading to an increase in the solute−ion interaction contribution to the total dynamic Stokes shift. The total temperature-induced change in the shift and the temperature coefficient of it predicted for these ionic liquids are in good agreement with the existing experimental results for either the same or nearly the same systems. In addition, the present calculations suggest that the fast component in the Stokes shift dynamics arises from the fast rotational relaxation of the dipolar ions of these liquids. This and the calculated magnitude of the dipole−dipole interaction contribution to the total shift substantiate the role of dipole−dipole interaction and orientational relaxation for the fluorescence spectral dynamics in these ionic liquids. The calculated average solvation times show a near proportionality to η/T which has also been observed earlier in experiments with several ionic liquids. Moreover, the activation energies obtained from the calculated solvation times are comparing well with the available experimental results for these liquids.

Although several predictions of the present work are in good agreement with the available experimental results, there exist several drawbacks. The first and most important is the complete

neglect of heterogeneity in solvent structure in these liquids. Because this factor was not incorporated systematically, the theory is unable to reveal why the average solvation times in ionic liquids exhibit a near proportionality relationship to η/T, even though in closely related systems (interaction-wise) a fractional power dependence has been experimentally observed.[51] Second, the liquid particles are assumed to be hard spheres with a point charge or point dipole at the center of those spheres. Considerations of more realistic shapes and charge distributions are therefore required for a better description of the static correlations of these complex liquids. The use of the mean spherical approximation (MSA) model for calculating these correlations might be inappropriate, but the low polarity of these liquids probably minimizes the nonlinearity effects. In fact, the Kirkwood correlation factors obtained from experiments[26] and simulations[71] involving ionic liquids do indicate that such a linearized description of dipole distribution may be valid for these complex liquids.

A recent theoretical study[72] indicated that the use of dipole moments as descriptors of several properties for ionic liquids might not be quite accurate, as the dipole moment of an ion is a coordinate-dependent quantity. Although this is a valid aspect for proper modeling of a given ionic liquid, the focus here was to uncover the possible role of dipolar interaction for Stokes shift dynamics in ionic liquids. In the present theory, the dipole moment is obtained from a statistical mechanical relation using the experimentally measured static dielectric constants of these liquids.[47] Interestingly, dipole moments obtained in this manner have been found to be very close to those obtained from more sophisticated quantum-chemical calculations. Note the above study[72] does not question the relevance of the dipole−dipole interaction in describing the Stokes shift dynamics in these liquids but does raise an issue regarding how quantitative that description would be. In addition, relevant research works[71] have indicated that the Madden−Kivelson relationship[73] between the collective and single-particle molecular dipole moment, which has been found successful in conventional polar liquids,[74] is also qualitatively valid in describing the dielectric spectra of ionic liquids. These pieces of evidence only suggest that the present framework is probably safe to describe, at least qualitatively, the Stokes shift dynamics in these liquids.

The calculations presented here on the temperature dependence of average solvation times may also be used to understand the role of nonrelaxational dynamics in the experimentally monitored time evolution of the fluorescence emission spectrum (of a dye molecule) in these ionic liquids at lower temperatures, particularly in the high viscosity ones.[67,75−79] It is known that dye molecules partitioned into different domains can have different decay rates, and this might produce an apparent shift in the fluorescence spectrum that does not have origin in the solvent relaxation. Because lowering of the temperature assists domain formation, the contribution of the inhomogeneous decay kinetics might not be negligible in ionic liquids at lower temperature, particularly for those with longer alkyl chains attached to cations. At very low temperature, where the solvent motions are expected to be nearly frozen, the inhomogeneous decay rate can provide a decay channel faster than that through environmental relaxation. As a result, the average rate of solvation measured in a conventional Stokes shift experiment will be higher than what it should be had only the solvent relaxation contributed. A comparison between theory and experiments in such cases might help in assessing the nonrelaxational contribution to the measured Stokes shift dynamics. The present theory could also be suitably extended to study the Stokes shift dynamics in binary mixtures of ionic liquids with polar solvents at room temperature or of two ionic liquids.[80−84] It would also be interesting to explore the relationship between the macroscopic and microscopic relaxation times in ionic liquids.[85] In the present theory, the dielectric relaxation data are used as inputs to the calculations of dynamics which actually carry information on macroscopic relaxation processes. Solvation processes, on the other hand, include relaxations at molecular length scales. Therefore, a possible link between the dielectric relaxation time and the single-particle orientational relaxation time in pure dipolar ionic liquids should be investigated.

Acknowledgment. H.K.K. thanks SNBNCBS, Kolkata, India, for a research fellowship. This article is dedicated to the fond memory of Dr. Suhrita Bagchi.

Supporting Information Available: Figures showing the time-dependent decays of various components of the solvation response functions calculated at different temperatures for several imidazolium ionic liquids and tables containing fit parameters. This material is available free of charge via the Internet at http://pubs.acs.org.

References and Notes

(1) Samanta, A. *J. Phys. Chem. Lett.* **2010**, *1*, 1557.
(2) Samanta, A. *J. Phys. Chem. B* **2006**, *110*, 13704.
(3) Arzhantsev, S.; Jin, H.; Baker, G. A.; Maroncelli, M. *J. Phys. Chem. B* **2007**, *111*, 4978.
(4) Ingram, J. A.; Moog, R. S.; Ito, N.; Biswas, R.; Maroncelli, M. *J. Phys. Chem. B* **2003**, *107*, 5926.
(5) (a) Weingartner, H. *Angew. Chem., Int. Ed.* **2008**, *47*, 654. (b) Krossing, I.; Slattery, J. M.; Daguenet, C.; Dyson, P. J.; Oleinikova, A.; Weingartner, H. *J. Am. Chem. Soc.* **2006**, *128*, 13427.
(6) Kobrak, M. N. *Adv. Chem. Phys.* **2008**, *139*, 83.
(7) Ionic Liquids. *Acc. Chem. Res.* **2007**, *40*, 1077 (special issue on ionic liquids).
(8) The Physical Chemistry of Ionic Liquids. *J. Phys. Chem. B* **2007**, *111*, 4639 (special issue on ionic liquids).
(9) Physical Chemistry of Ionic Liquids. *Phys. Chem. Chem. Phys.* **2010**, *12*, 1629 (special issue on ionic liquids).
(10) *Indian J. Chem.* **2010**, *49A*, 635 (special issue on ionic liquids).
(11) Plechkova, N. V.; Seddon, K. R. *Chem. Soc. Rev.* **2008**, *37*, 123.
(12) Rogers, R. D.; Seddon, K. R. *Ionic Liquids: Industrial Applications to Green Chemistry*; ACS Symposium Series 818; American Chemical Society: Washington, DC, 2002.
(13) Wasserscheid, P.; Welton, T. *Ionic Liquids in Synthesis*; Wiley-VCH: New York, 2003.
(14) Jin, H.; Baker, G. A.; Arzhantsev, S.; Dong, J.; Maroncelli, M. *J. Phys. Chem. B* **2007**, *111*, 7291.
(15) Wang, Y.; Voth, G. A. *J. Am. Chem. Soc.* **2005**, *127*, 12192.
(16) Triolo, A.; Russina, O.; Bleif, H.; Cola, E. D. *J. Phys. Chem. B* **2007**, *111*, 4641.
(17) (a) Mandal, P. K.; Sarkar, M.; Samanta, A. *J. Phys. Chem. A* **2004**, *108*, 9048. (b) Sarkar, A.; Trivedi, S.; Baker, G. A.; Pandey, S. *J. Phys. Chem. B* **2008**, *112*, 14927. (c) Bhargava, B. L.; Klein, M. L.; Balasubramanian, S. *ChemPhysChem* **2008**, *9*, 67.
(18) Jin, H.; Li, X.; Maroncelli, M. *J. Phys. Chem. B* **2007**, *111*, 13473.
(19) Adhikari, A.; Sahu, A. K.; Dey, S.; Ghose, S.; Mandal, U.; Bhattacharyya, K. *J. Phys. Chem. B* **2007**, *111*, 12809.
(20) Hu, Z.; Margulis, C. J. *Proc. Natl. Acad. Sci. U.S.A.* **2006**, *103*, 831.
(21) Lopes, J. A. C.; Padua, A. A. H. *J. Phys. Chem. B* **2006**, *110*, 3330.
(22) Arzhantsev, S.; Ito, N.; Heitz, M.; Maroncelli, M. *Chem. Phys. Lett.* **2003**, *381*, 278.
(23) Nagasawa, Y.; Oishi, A.; Itoh, T.; Yasuda, M.; Muramatsu, M.; Ishibashi, Y.; Ito, S.; Miyasaka, H. *J. Phys. Chem. C* **2009**, *113*, 11868.
(24) Funston, A.; Fadeeva, T. A.; Wishart, J. A.; Castner, E. W. *J. Phys. Chem. B* **2007**, *111*, 4963.
(25) Frauchey, K.; Fayer, M. D. *J. Phys. Chem. B* **2010**, *114*, 2840.
(26) Wulf, A.; Ludwig, R.; Sasisanker, P.; Weingartner, H. *Chem. Phys. Lett.* **2007**, *439*, 323.
(27) Mizoshiri, M.; Nagao, T.; Mizoguchi, Y.; Yao, M. *J. Chem. Phys.* **2010**, *132*, 164510.
(28) Hunger, J.; Stoppa, A.; Schrodle, S.; Hefter, G.; Buchner, R. *Chem. Phys. Chem.* **2009**, *10*, 723.
(29) Kashyap, H. K.; Biswas, R. *J. Phys. Chem. B* **2008**, *112*, 12431.

(30) Kashyap, H. K.; Biswas, R. *J. Phys. Chem. B* **2010**, *114*, 254.
(31) Kashyap, H. K.; Biswas, R. *Indian J. Chem.* **2010**, *49A*, 685.
(32) Bagchi, B.; Biswas, R. *Adv. Chem. Phys.* **1999**, *109*, 207.
(33) Roy, S.; Bagchi, B. *J. Chem. Phys.* **1993**, *99*, 9938.
(34) Roy, S.; Bagchi, B. *J. Chem. Phys.* **1993**, *99*, 1310.
(35) Nandi, N.; Roy, S.; Bagchi, B. *J. Chem. Phys.* **1995**, *102*, 1390.
(36) Biswas, R.; Bagchi, B. *J. Phys. Chem. B* **1996**, *100*, 1238.
(37) Horng, M. L.; Gardecki, J. A.; Papazyan, A.; Maroncelli, M. *J. Phys. Chem.* **1995**, *99*, 17311.
(38) Chapman, C. F.; Maroncelli, M. *J. Phys. Chem.* **1991**, *95*, 9095.
(39) Tokuda, H.; Tsuzuki, S.; Susan, M. A. B. H.; Hayamizu, K.; Watanabe, M. *J. Phys. Chem. B* **2006**, *110*, 19593.
(40) MacFarlane, D. R.; Forsyth, M.; Izgorodina, E. I.; Abbott, A. P.; Annat, G.; Fraser, K. *Phys. Chem. Chem. Phys.* **2009**, *11*, 4962.
(41) (a) Chandra, A.; Wei, D.; Patey, G. N. *J. Chem. Phys.* **1993**, *98*, 4959. (b) Chandra, A.; Wei, D.; Patey, G. N. *J. Chem. Phys.* **1993**, *99*, 2083. (c) Chandra, A.; Patey, G. N. *J. Chem. Phys.* **1994**, *100*, 1552.
(42) Chandra, A. *Chem. Phys. Lett.* **1995**, *244*, 314.
(43) Chandra, A.; Jana, D.; Bhattacharjee, S. *J. Chem. Phys.* **1996**, *104*, 8662.
(44) Mahajan, K.; Chandra, A. *J. Chem. Phys.* **1997**, *106*, 2360.
(45) Bagchi, B.; Chandra, A. *Adv. Chem. Phys.* **1991**, *80*, 1.
(46) Bagchi, B. *Annu. Rev. Phys. Chem.* **1989**, *40*, 115.
(47) Gray, C. G.; Gubbins, K. E. *Theory of Molecular Fluids*; Clarendon: Oxford, U.K., 1984; Vol. I.
(48) Jin, H.; O'Hare, B.; Arzhantsev, S.; Baker, G.; Wishart, J. F.; Binesi, A. J.; Maroncelli, M. *J. Phys. Chem. B* **2008**, *112*, 81.
(49) Bhargava, B. L.; Balasubramanian, S. *J. Phys. Chem. B* **2007**, *111*, 4477.
(50) Hansen, J. P.; McDonald, I. R. *Theory of Simple Liquids*, Academic Press: San Diego, CA, 1986.
(51) Guchhait, B.; Gazi, H. A. R.; Kashyap, H. K.; Biswas, R. *J. Phys. Chem. B* **2010**, *114*, 5066.
(52) Attard, P. *Phys. Rev. E* **1993**, *48*, 3604.
(53) Chandra, A.; Bagchi, B. *J. Chem. Phys.* **1999**, *110*, 10024.
(54) Bagchi, B. *J. Chem. Phys.* **1994**, *100*, 6658.
(55) Reynolds, L.; Gardecki, J. A.; Frankland, S. J.; Horng, M. L.; Maroncelli, M. *J. Phys. Chem.* **1996**, *100*, 10337.
(56) Ito, N.; Arzhantsev, S.; Maroncelli, M. *Chem. Phys. Lett.* **2004**, *396*, 83.
(57) Khupse, N. D.; Kumar, A. *J. Phys. Chem. B* **2010**, *114*, 376.
(58) Lee, J. M.; Ruckes, S.; Prasunitz, J. M. *J. Phys. Chem. B* **2008**, *112*, 1473.
(59) Martins, C. T.; Sato, B. M.; El Seoud, O. A. *J. Phys. Chem. B* **2008**, *112*, 8330.
(60) Baker, S. N.; Baker, G. A.; Bright, F. V. *Green Chem.* **2002**, *4*, 165.
(61) Reichardt, C. *Chem. Rev.* **1994**, *94*, 2319.
(62) Lakowicz, J. R. *Principles of Fluorescence Spectroscopy*; Plenum Press: New York, 1983.
(63) (a) Turton, D. A.; Hunger, J.; Stoppa, A.; Hefter, G.; Thoman, A.; Walther, M.; Buchner, R.; Wynne, K. *J. Am. Chem. Soc.* **2009**, *131*, 11140. (b) Fujisawa, T.; Nishikawa, K.; Shirota, H. *J. Chem. Phys.* **2009**, *131*, 2009. (c) Giraud, G.; Gordon, C. M.; Dunkin, I. R.; Wynne, K. *J. Chem. Phys.* **2003**, *119*, 464. (d) Shirota, H.; Funston, A. M.; Wishart, J. F.; Castner, E. W., Jr. *J. Chem. Phys.* **2005**, *122*, 184512. (e) Shirota, H.; Castner, E. W., Jr. *J. Phys. Chem. A* **2005**, *109*, 9388. (f) Shirota, H.; Castner, E. W., Jr. *J. Phys. Chem. B* **2005**, *109*, 21576. (g) Hyun, B.-R.; Dzyuba, S. V.; Bartsch, R. A.; Quitevis, E. L. *J. Phys. Chem. A* **2002**, *106*, 7579.
(64) Hu, Z.; Huang, X.; Annapureddy, H. V. R.; Margulis, C. *J. Phys. Chem. B* **2008**, *112*, 7837.
(65) Kashyap, H. K.; Pradhan, T.; Biswas, R. *J. Chem. Phys.* **2006**, *125*, 174506.
(66) Ito, N.; Arzhantsev, S.; Heitz, M.; Maroncelli, M. *J. Phys. Chem. B* **2004**, *108*, 5771.
(67) Fee, R. S.; Milsom, J. A.; Maroncelli, M. *J. Phys. Chem.* **1991**, *95*, 5170.
(68) Roy, D.; Mondal, S. K.; Sahu, K.; Ghosh, S.; Sen, P.; Bhattacharyya, K. *J. Phys. Chem. A* **2005**, *109*, 7359.
(69) Sen, P.; Mukherjee, S.; Halder, A.; Bhattacharyya, K. *Chem. Phys. Lett.* **2004**, *385*, 357.
(70) Pramanik, R.; Rao, V. G.; Sarkar, S.; Ghatak, C.; Setua, P.; Sarkar, N. *J. Phys. Chem. B* **2009**, *113*, 8626.
(71) Schroder, C.; Wakai, C.; Weingartner, H.; Steinhauser, O. *J. Chem. Phys.* **2007**, *126*, 084511.
(72) Kobrak, M. N.; Li, H. *Phys. Chem. Chem. Phys.* **2010**, *12*, 1922.
(73) Madden, P.; Kivelson, D. *Adv. Chem. Phys.* **1984**, *56*, 467.
(74) Ravichandran, S.; Bagchi, B. *Int. Rev. Phys. Chem.* **1995**, *14*, 271.
(75) Maroncelli, M.; Fee, R. S.; Chapman, C. F.; Fleming, G. R. *J. Phys. Chem.* **1991**, *95*, 1012.
(76) Kinoshita, S.; Nishi, N. *J. Chem. Phys.* **1988**, *89*, 6612.
(77) Campbell, B. F.; Chance, M. R.; Friedman, J. M. *Science* **1987**, *238*, 373.
(78) Agmon, N. *Biochemistry* **1988**, *27*, 3507.
(79) Agmon, N. *J. Phys. Chem.* **1990**, *94*, 2959.
(80) (a) Chakrabarty, D.; Chakraborty, A.; Seth, D.; Hazra, P.; Sarkar, N. *Chem. Phys. Lett.* **2004**, *397*, 469. (b) Sarkar, S.; Pramanik, R.; Ghatak, C.; Setua, P.; Sarkar, N. *J. Phys. Chem. B* **2010**, *114*, 2779. (c) Chakrabarty, D.; Chakraborty, A.; Seth, D.; Sarkar, N. *J. Phys. Chem. A* **2005**, *109*, 1764.
(81) Hunger, J.; Stoppa, A.; Buchner, R.; Hefter, G. *J. Phys. Chem. B* **2009**, *113*, 9527.
(82) Stoppa, A.; Buchner, R.; Hefter, G. *J. Mol. Liq.* **2010**, *153*, 46.
(83) Xiao, D.; Rajian, J. R.; Li, S.; Bartsch, R. A.; Quitevis, E. L. *J. Phys. Chem. B* **2006**, *110*, 16174.
(84) Xiao, D.; Rajian, J. R.; Hines, S.; Li, S.; Bartsch, R. A.; Quitevis, E. L. *J. Phys. Chem. B* **2008**, *112*, 13316.
(85) Chandra, A.; Bagchi, B. *J. Phys. Chem.* **1990**, *94*, 3152.

JP106271N